Chapter 3

The Major Cause of Earthquake Disasters: Shear Bandings

Tse-Shan Hsu

Additional information is available at the end of the chapter

http://dx.doi.org/10.5772/intechopen.74718

Abstract

In the last two decades, due to disasters happening around the world have been recorded precisely. People have begun to understand that earthquakes fall under several categories. Most of the earthquake-induced catastrophes, including fallen bridges, building collapses, soil liquefaction, and landslides, can only appear in shear banding zones induced by tectonic earthquakes. It is important to mention that tectonic earthquakes are different from other earthquakes because, in addition to the seismic vibration effect present in all earthquakes, tectonic earthquakes have a shear banding effect. In a tectonic earthquake, the shear banding energy can be more than 90% of the total earthquake energy, and the primary cause of earthquake disasters is the presence of the shear banding. In the past, the cause of earthquake disasters has been generally identified by structure dynamics researchers, without any proof, as the insufficiency of seismic-vibration resistant forces. Therefore, the modification of building codes and specifications has only focused on increasing these resistance forces. However, this type of specification modification cannot guarantee that an earthquake-resistant design structure would not fail due to shear banding. Thus, it is the objective of this study to present appropriate earthquake disaster prevention methods for a tectonic earthquake.

Keywords: tectonic earthquake, disaster, shear banding, seismic-vibration, major effect

1. Introduction

The China Earthquake Disaster Prevention Center [1] pointed out that earthquakes can be divided into five different types, namely, tectonic earthquakes, volcanic earthquakes, collapse earthquakes, induced earthquakes, and artificial earthquakes. Of these, tectonic earthquakes

are the most prevalent, accounting for about 90% of the total number of earthquakes around the world. Their destructive power is also the strongest.

Due to the mutual interaction of tectonic plates, lateral compression or lateral extension phenomena may exist. Once the shear strain enters the plastic range, Drucker [2], Hill [3], Mandel [4], Rice [5], Rudnicki and Rice [6], and Valanis [7] addressed that the localization of deformations will appear due to the loss of ellipticity, and further derived the shear bands shown in **Figure 1**.

During shear banding, excess pore water pressure is highly concentrated in a shear band, as shown in **Figure 2**. In addition, repeated stick-slip phenomena will be induced, as shown in **Figure 3**. When the sticking action continues to raise the friction resistance up to the maximum value of the static friction resistance, the sticking phenomenon will then change to slipping. At this point in time, the friction resistance changes from static friction to kinetic friction. While the slipping action continues until the sticking reappears, the friction resistance will drop to the minimum value of the kinetic friction resistance. Thereafter, the static friction resistance will increase again. When the stick-slip phenomenon repeatedly appears in shear bandings, and the

Figure 1. An actual shear band and numerical simulation results [8]: (a) an actual shear band that occurred in Zhushan, Taiwan, during the 921 Jiji earthquake; (b) shear bands produced by the finite element method.

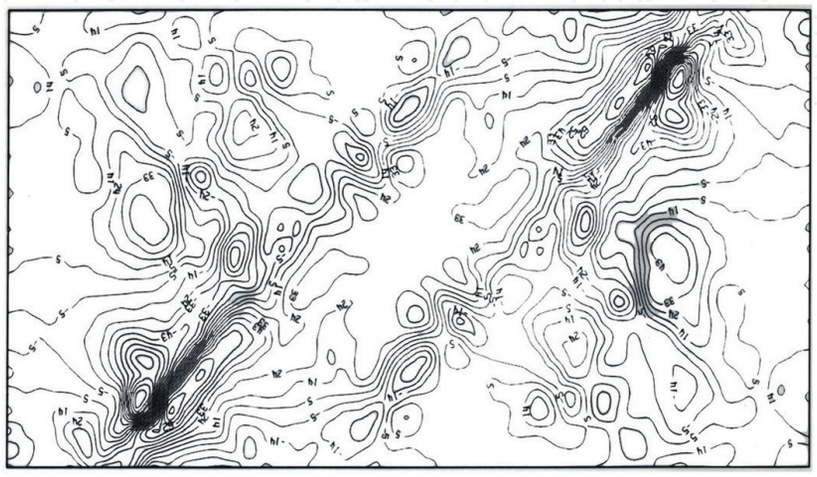

Figure 2. Contours of excess pore water pressures related to **Figure 1b** [8].

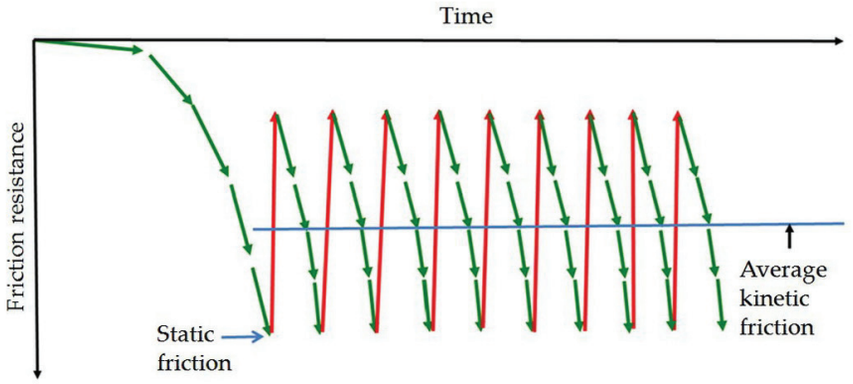

Figure 3. Stick-slip phenomenon in shear banding (modified from [9]).

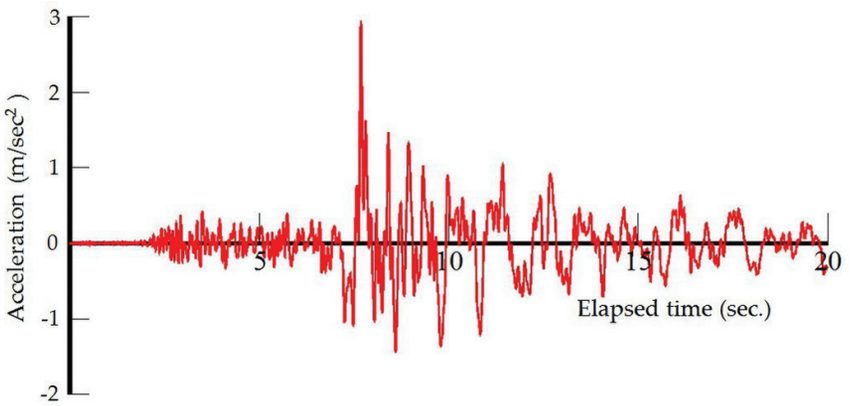

Figure 4. Seismometer record of the ground acceleration time-history curve.

state changes from sticking to slipping, the shear banding will accelerate; conversely, when the state changes from slipping to sticking, the shear banding will decelerate. Therefore, in shear banding, the ground acceleration time-history curve, as shown in **Figure 4**, can be recorded by a seismometer installed on the ground surface.

It can be concluded from **Figures 1** to **4** that: (1) shear bands are induced by applying lateral compression or lateral extension on a tectonic plate; (2) highly concentrated excess pore water pressure can be induced in a shear band; and (3) ground vibration is induced by shear banding. Thus, the primary cause of earthquake disasters is shear banding.

2. Bridge disaster caused by shear banding

Figure 5a shows the Jianmin bridge which collapsed during the Jiji earthquake. **Figure 5b** shows the rebuilt bridge in 2001 using the new seismic zone division updated in 1999. During Typhoon Fanapi in 2010, the new bridge collapsed again (details in **Figure 5c**). **Figure 5d** shows that the bridge was rebuilt again in 2012 using the new seismic zone divisions updated in 2005. **Figure 5e** shows the exposed pile cap of the bridge only two months after reconstruction.

Figure 5. History of the Jianmin bridge in Taichung, Taiwan: (a) bridge collapsed during the Jiji earthquake, 1999 [10]; (b) bridge rebuilt in 2001 [11]; (c) bridge collapsed again in 2010; (d) bridge rebuilt again in 2012; (e) the exposed pile cap of the bridge [12].

Figure 5a clearly shows that the riverbed around the Jianmin bridge was seriously fractured during the Jiji earthquake. **Figure 6** indicates the shear textures, including the principal deformation shear, D; the thrust shear, P; the Riedel shear, R; the conjugated Riedel Shear, R'; and the compression texture, S, in the total width of a shear band. Thus, even though the vibration resistance forces were increased, both the old and new Jianmin bridge collapsed due to the effects of shear banding.

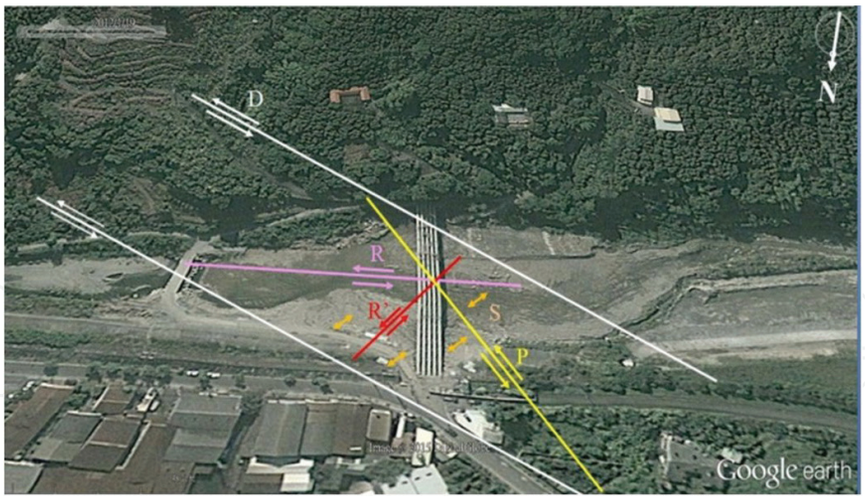

Figure 6. A shear band near the Jianmin bridge (background satellite image was cited from [11]).

3. Building disasters caused by shear banding

3.1. Case study 1

After the 921 Jiji earthquake, Kuangfu Junior High School in Taichung was maintained as an earthquake memorial museum for shear banding, ground uplift, and school building collapse, thereby, preserving the historical facts of the earthquake and providing students and the public educational earthquake material. In 2001, the school was renamed as the 921 Earthquake Education Park. Although the establishment of the museum is well intentioned, the explanations within the museum do not discuss the primary effect, and thus it is difficult to achieve the desired educational function. Taking the Kuangfu Junior High School building as an example, the building collapse is depicted in **Figure 7**. The actual mechanism for such a localized collapse, shown in **Figure 8**, was the occurrence of shear banding during a tectonic earthquake. However, under the guidance of the park instructor, currently, the students and members of the public who have visited consider that the primary cause of the building collapse was the excessive seismic vibration.

Figure 7. The collapse of the Kuangfu junior high school building during the Jiji earthquake: (a) front view; (b) rear view.

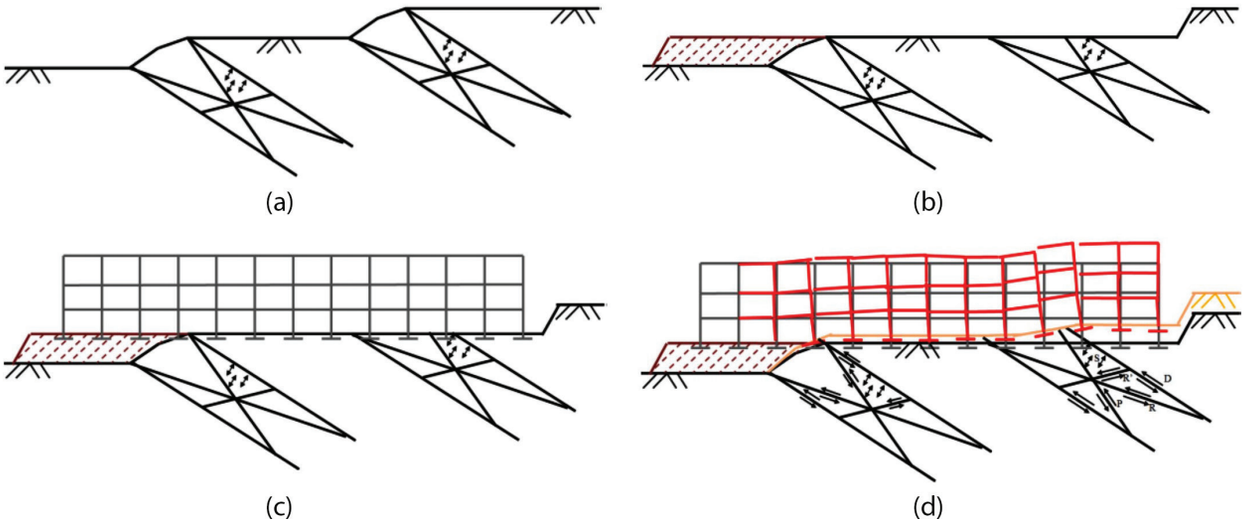

Figure 8. Schematic diagrams of the building construction process and collapse mechanism: (a) tilted slopes caused by shear banding; (b) ground leveling; (c) building constructed on shear bands; and (d) building collapsed by shear banding.

It is to be stressed that this kind of discourse makes it difficult for people to understand why there are buildings left intact by the same earthquake within the school district.

With this in mind, correctly stipulating and amending the seismic design specifications of buildings and correctly executing earthquake education are both required to guarantee that buildings will remain stable during tectonic earthquakes, with magnitudes less than the design magnitude.

3.2. Case study 2

The Weiguan building was completed in 1994. It remained stable during the Jiasian tectonic earthquake with a magnitude of M_L = 6.4 in 2010 (refer to **Figure 9a**), but collapsed during the magnitude M_L = 6.4 Meinong tectonic earthquake in 2016 (refer to **Figure 9b**).

Figure 9. The Weiguan building: (a) before the collapse [11]; (b) after the collapse [13].

It was found from the monitor record images that before the collapse of the Weiguan building, a 2 m diameter pipe burst in the tap-water supply trunk pipe, embedded under the road adjacent to the building. After the pipe burst, a hole with a 4 m depth suddenly appeared. Because of the sudden appearance of the hole, the conditions of the side walls surrounding the basement, previously constrained, were partially unconstrained.

Since the soil under the road was sandy silt, such a soil layer still retained considerably high shear force resistance in a dry state, which caused Block G to recline on the road's ground surface after the collapse of the Weiguan building (details in **Figure 10**). In addition, sandy silt shear resistance strength drops significantly in a saturated state, which caused Block A to fall 2.5 m deep into the ground after the collapse. When the soil under the road adjacent to Block A lost lateral support, the bottoms of all the columns in the first floor deviated from the fixed end conditions established in the structural analysis model.

As for the cause of the damage to the large-scale water supply pipe, Liu [14] and Hsu et al. [15] pointed out that the peak ground acceleration (PGA) was not the main cause for its damage during the earthquake; the main cause was shear banding. From this, we can conclude that the bursting of the tap-water supply trunk pipe on the road adjacent to the Weiguan building was actually mainly caused by shear banding.

3.3. Procedure for building failure identification

Since tectonic earthquakes are the most prevalent and their destructive power is also the strongest, all earthquakes that cause major disasters are tectonic earthquakes. A procedure for the identification of building failures that occurred in a tectonic earthquake is proposed as follows:

Step 1: Ensure that the earthquake is a tectonic earthquake.

Step 2: Use satellite images, GPS velocity vectors, or in situ topography features to find the locations of shear bands.

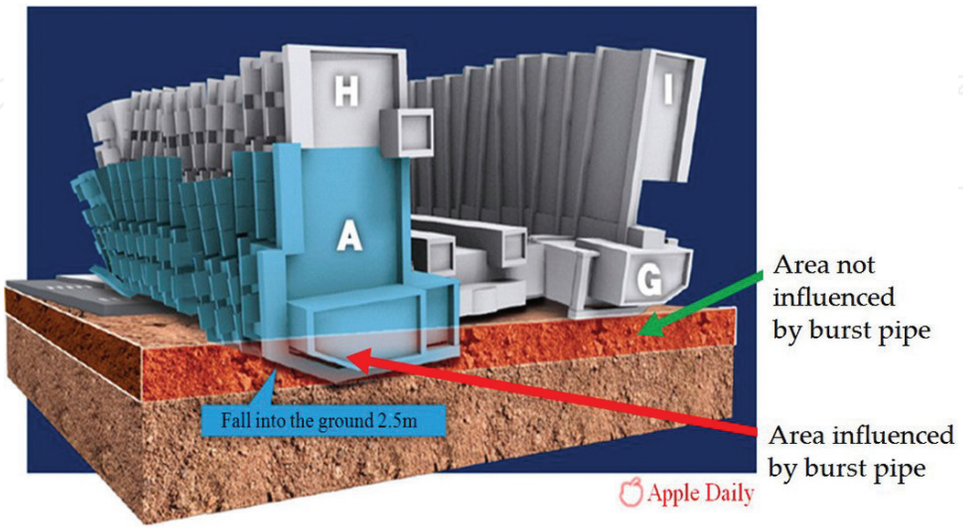

Figure 10. Schematic diagram of the Weiguan building after the collapse [16].

Step 3: If shear banding is located under the foundation of the building, the reason for causing the failure is directly related to the shear banding.

Step 4: If shear banding is located near the building, the cause can be found only after conducting a structural dynamic analysis for a structural model of the whole building, subjected to the effects of both shear banding and seismic vibration.

Step 5: If the building failure did not occur in a previous tectonic earthquake, the cause of the failure can only be found after identifying the differences in conditions between the first and second tectonic earthquake.

3.4. Application of the procedure for building failure identification

The above-listed procedure is applied to the Weiguan building as follows:

Step 1: The collapse of the Weiguan building occurred during the Meinong earthquake, which has been proven by the Taiwanese Central Weather Bureau to be a tectonic earthquake.

Step 2: The GPS velocity vectors shown in **Figure 11** indicate that shear banding did occur near the Weiguan building. The pipe burst is another piece of evidence for shear banding.

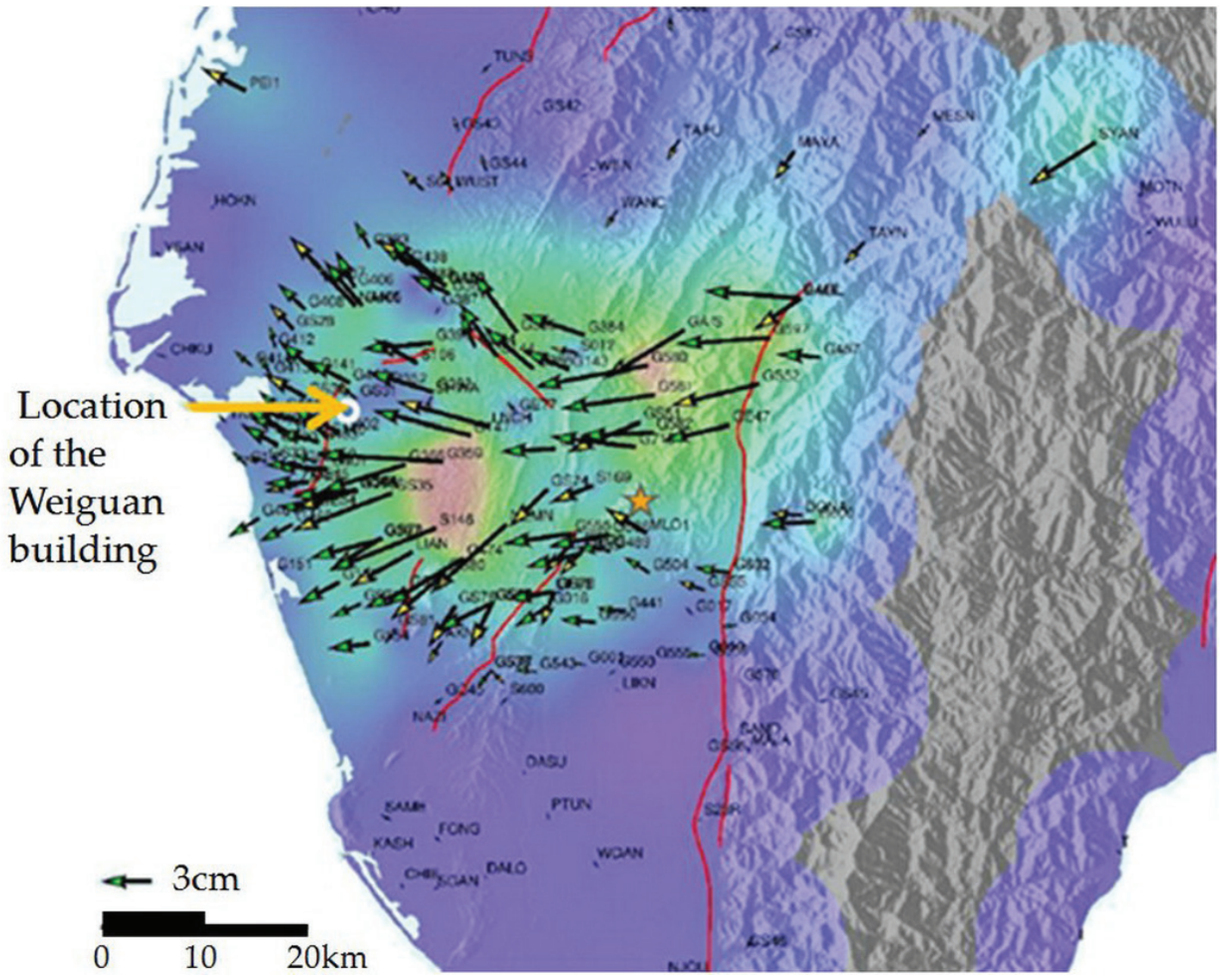

Figure 11. The GPS velocity vectors produced by the Meinong earthquake [17].

http://dx.doi.org/10.5772/intechopen.74718

Note, however, that such a shear banding phenomenon did not occur during the 2010 Jiasian earthquake.

Steps 3–5: Since shear banding near the Weiguan building did not occur in the 2010 Jiasian earthquake, but did occur in the 2016 Meinong earthquake, a structural dynamic analysis for a structural model of the whole building subjected to the seismic vibration effects with or without the shear banding effect is conducted.

A structural model of the whole building, including all elements of both the upper and the lower structures, is used, as shown in **Figure 12**. It is important to mention that the cross sections and material properties used in the analyses are similar to those adopted by the original designer. The side walls surrounding the basement are constrained by springs, with their elastic modulus determined by values of N from standard penetration tests. When the pipe burst is to be considered (or not considered), the springs for the side walls near the pipe burst area are removed (or not removed), such that the effect of shear banding can be determined numerically. The loading conditions included both static loads and seismic vibration forces; the static loads include a live load 200 kgf/m^2 and a dead load 150 kgf/m^2, in addition to the body forces of the structural elements. The seismic vibration forces are generated by the acceleration history taken from Station No. CHY063, as shown in **Figure 13**.

Since the major concern for the Weiguan building disaster is that the whole building initially tilted toward the X-direction near the bottom joints of the first floor, the numerical results focus on the four nodes shown in **Figure 14**.

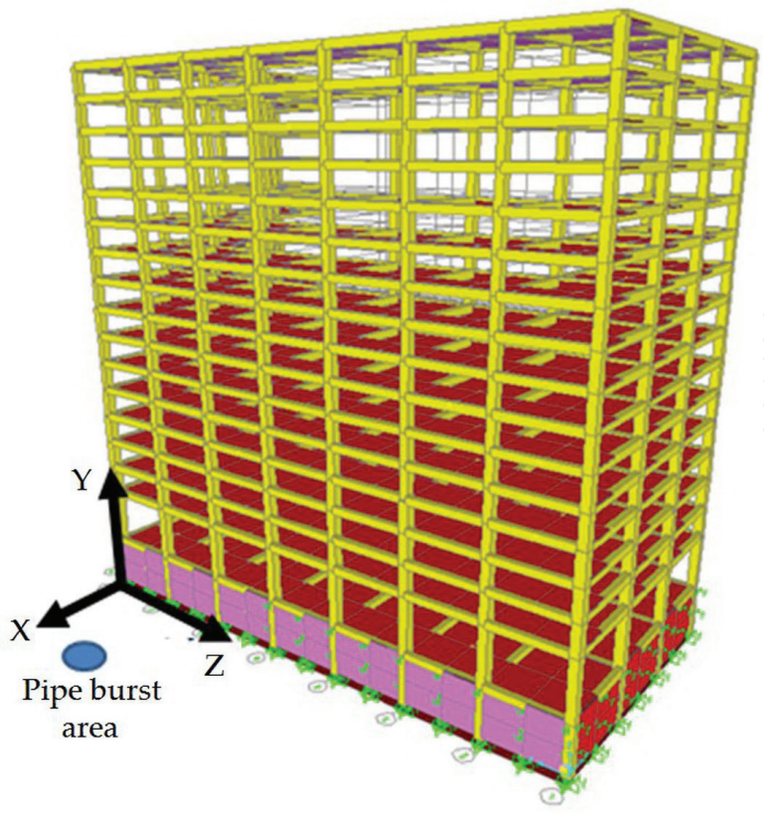

Figure 12. The structural model used in the dynamic analyses.

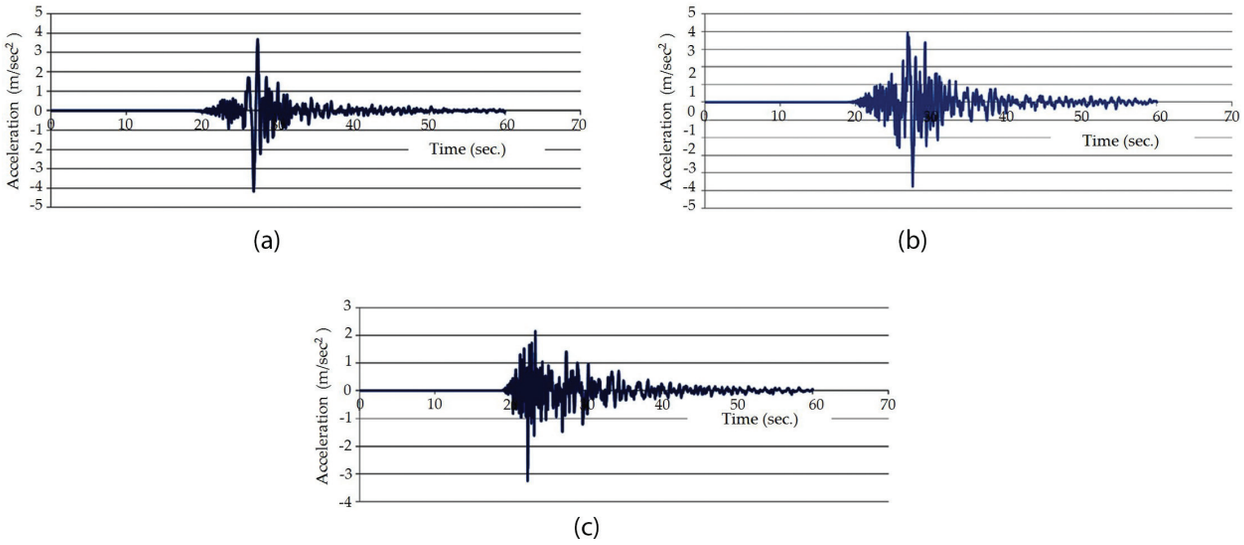

Figure 13. The acceleration history adopted in the analyses [18]: (a) X-direction; (b) Y-direction; (c) Z-direction.

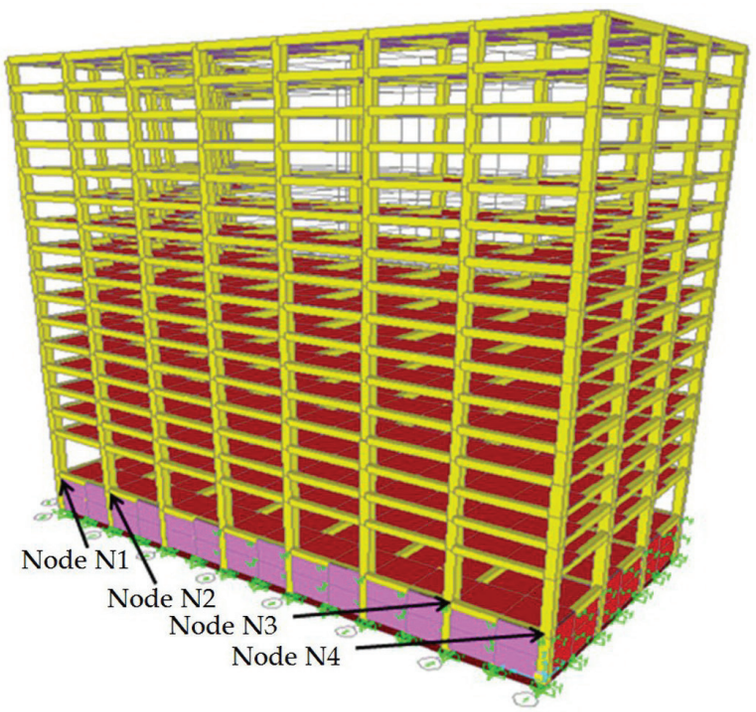

Figure 14. The four major nodes of concern in the structure model.

The maximum displacements for the four joints shown in **Figure 14** from the structure dynamic analyses with and without the shear banding effect are shown in **Table 1**. Case 1 includes the shear banding effect and Case 2 does not.

Since no failure occurred during the 2010 Jiasian earthquake, the results of Case 2 are considered to be the displacement safety values. Whether the results of Case 1 can be used as safety values will depend on the fraction, F_{12} calculated by dividing the displacements of Case 1 by

Node number	Maximum displacement during a tectonic earthquake (cm)							
	X-direction component		Y-direction component		Z-direction component		Total vector	
	Case 1	Case 2	Case 1	Case 2	Case 1	Case 2	Case 1	Case 2
N1	13.85	7.09	9.08	3.96	12.21	7.98	20.57	11.38
N2	9.15	4.44	9.01	4.11	8.92	5.50	15.63	8.34
N3	4.99	4.45	7.37	4.12	5.44	5.61	10.43	8.26
N4	8.12	7.09	7.00	3.96	7.73	8.02	13.21	11.41

Table 1. Numerical results for the structural model with and without the shear banding effect.

Node number	X-direction component	Y-direction Component	Z-direction component	Total vector
N1	1.95	2.29	1.53	1.81
N2	2.06	2.19	1.62	1.87
N3	1.12	1.79	0.97	1.26
N4	1.15	1.77	0.96	1.16

Table 2. Calculated values of fraction, F_{12}.

those of Case 2. The resulting F_{12} fractions are shown in **Table 2**. From **Table 2**, the shear banding effect is very significant for nodes N1 and N2 and less significant for nodes N3 and N4.

It should be mentioned that only for values of F_{12} of less than about 1.4, for the total displacement vector, will the building structure remain under stable conditions. However, the largest value of F_{12} for the total displacement vectors is 1.87. Since the worst conditions occurred at nodes N2 and N1, the tilting of the Weiguan building should begin from the side that was more under the influence of shear banding. Afterward, the tilting quickly propagated to the other side.

4. Soil liquefaction disaster caused by shear banding

Soil liquefaction will result in building damage during an earthquake. Thus, design engineers must carry out evaluations of the potential of soil liquefaction. For different locations with identical horizontal seismic coefficient, k_h, geological condition, and groundwater table, the results of conventional liquefaction potential evaluations will be the same. Taking Tainan City, Taiwan as an example, with $k_h = 0.33$ and the groundwater table close to the ground surface, the conventional soil liquefaction potential diagram published by the Central Geological Survey, MOEA is as shown in **Figure 15**. **Figure 15** reveals that all areas covered by the alluvial soil layer in Tainan City have high, moderate, or low soil liquefaction potential.

The actual location of soil liquefaction in Tainan City took place during the Meinong Earthquake on February 6, 2016, as shown in **Figure 16**. **Figure 16** also shows that: (1) soil liquefaction is

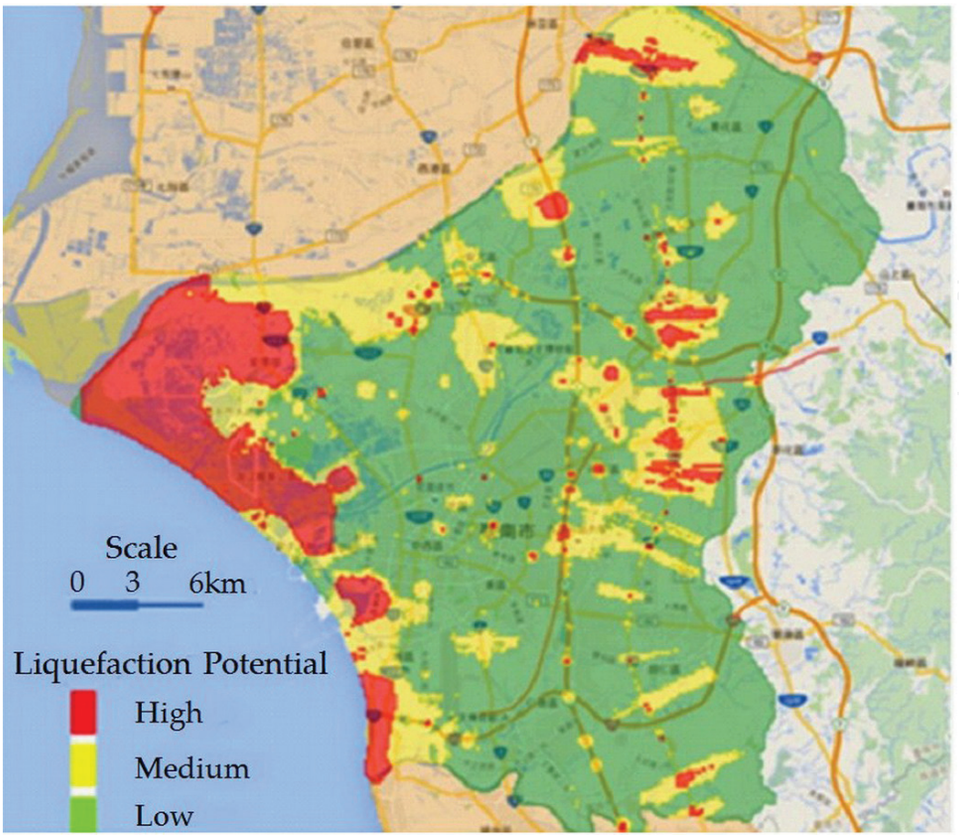

Figure 15. Conventional distribution of soil liquefaction potentials in Tainan, Taiwan [8, 19].

merely a kind of localized phenomenon; (2) the actual area of soil liquefaction is far less than the area of conventional soil liquefaction potential proposed by the Central Geological Survey, MOEA; and (3) the actual locations of soil liquefaction were mostly outside the areas with high liquefaction potential. Thus, we know that the conventional cause of soil liquefaction is different than the cause of localizations of soil liquefaction.

Localizations of soil liquefaction can be divided into tubular soil liquefaction and striped soil liquefaction. Tubular soil liquefaction results from a tectonic plate equipped with tubular water channels, similar to piping [20]. Hsu and Chiu [21] believed that this tubular water channel is formed by the intersection of shear textures of different strikes. Meanwhile, the striped soil liquefaction results from a tectonic plate equipped with striped water channels, which is the shear band under plane strain conditions (as shown in **Figure 1b**).

As for areas adjacent to soil liquefaction areas, even though they have identical conditions, the localizations of soil liquefaction do not exist because highly concentrated excess pore water pressure and groundwater channels were not induced during the earthquake.

Causes of localizations of soil liquefaction include: (1) high shear resistance of foundation soil led to strain softening behavior; (2) shear banding led to tectonic local uplift of the ground surface; (3) loosening of the shear band soil due to brittle fractures; (4) the expanded pore space of the shear band soil becomes the channel for upward groundwater flow with fragment entrainment; and (5) the upward flowing water with fragment entrainment will further loosen the shear band soil.

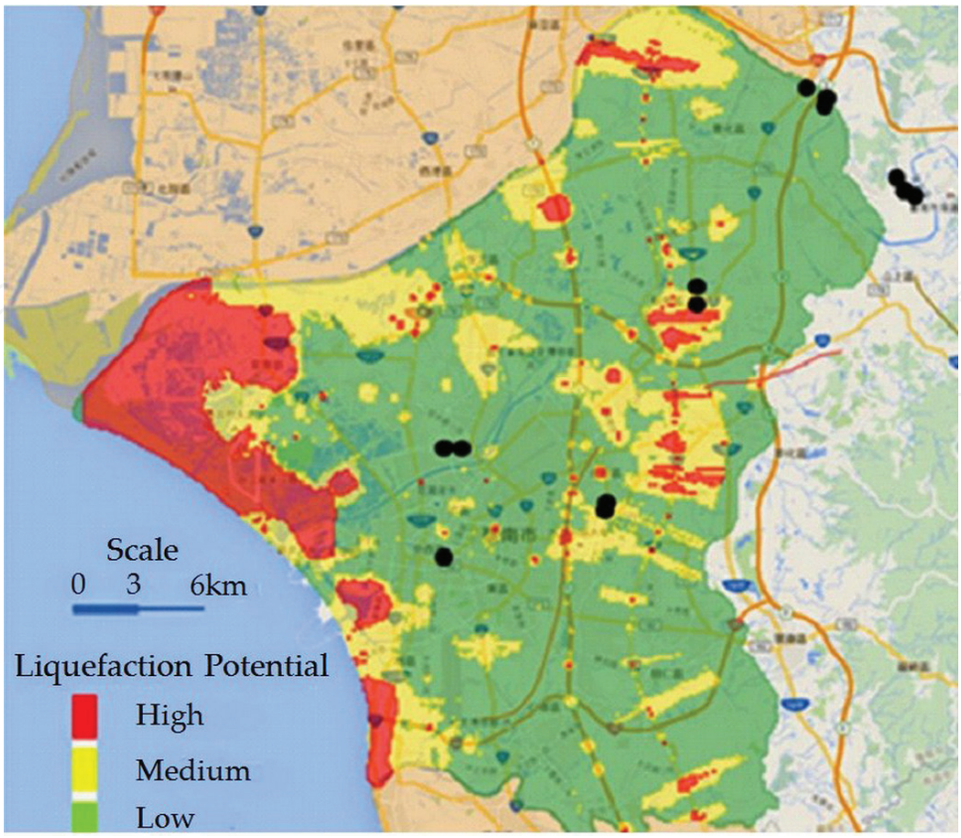

Figure 16. Comparison between the locations of soil liquefactions induced by the Meinong earthquake and the distribution of conventional liquefaction potential [8, 19].

A comparison of the various causes of conventional and localizations of soil liquefaction is shown in **Table 3**. It appears that the cause of conventional soil liquefaction is completely different from the cause of localizations of soil liquefaction. Obviously, the cause of localizations of soil liquefaction corresponds more closely to those of actual soil liquefaction.

	Conventional soil liquefaction	**Localizations of soil liquefaction**
Soil conditions	Loose or perfectly plastic	Dense or strain softening
Type of earthquakes causing soil liquefactions	Not specified	Tectonic earthquake
Inducing factor for the excess pore water pressure	All-around vibrations	Localizations of deformations
Change of soil conditions	All soil changed from a loose state to a dense state	Only the shear band soil is changed from a dense state to a loose state
Highly concentrated excess pore water pressure	Does not exist	Exists in shear bands
Discharged water path for groundwater to flow upward	Does not exist	The expanded pore space in the shear band soil

Table 3. Comparison among various causes of conventional soil liquefaction and localizations of soil liquefaction [8].

The building collapse pattern induced by localizations of soil liquefaction during a tectonic earthquake is shown in **Figure 17**. This kind of damage pattern is totally different from the pattern caused by foundation punching shear failure or local shear failure.

Different damage patterns will require different disaster prevention methods, so the building damage induced by foundation punching shear failure or local shear failure must not be misidentified as soil liquefaction damage.

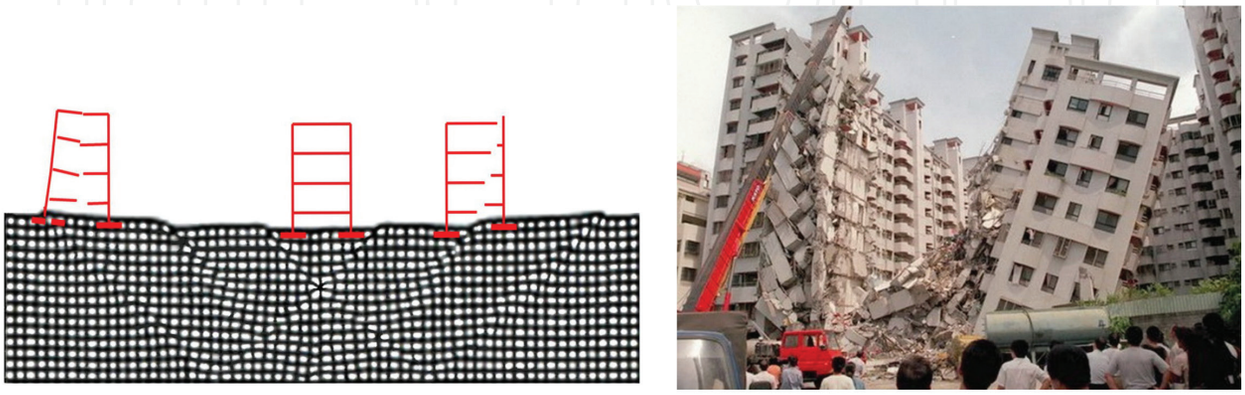

Figure 17. Building disaster caused by localizations of soil liquefaction during the Jiji earthquake, 1999: (a) schematic diagram of the building collapse pattern; (b) actual building collapse pattern [22].

Type of liquefaction	Prevention methods	
Conventional soil liquefaction [23]	Method 1. Building's design follows the revised standard of building earthquake resistance design, created on Dec. 29, 1999	
	Method 2. Foundation of the building located in non-liquefaction stratum (such as a clay layer, a gravel layer, or a bedrock, etc.)	
	Method 3. Buildings with more than three floors of basement	
	Method 4. The building foundation is of the pile type	
	Method 5. Buildings with mat foundation or buildings not higher than three floors	
Localizations of soil liquefaction	Shear banding liquefaction area	Step 1: Ensure that shear banding does not reach the ultimate bearing capacity area. Verification tests can be conducted on a faulting table to confirm that the shear banding is compensated in each layer of synthetic block. After that all shear banding should be compensated by design.
		Step 2: Calculate the bearing capability of the foundation under the designed tectonic plate vibration conditions during an earthquake. Make sure the safety factor of the foundation bearing capability under earthquake conditions is $FS_E \geqq 1.2$.
	Non-shear banding liquefaction area	Calculate the bearing capability of the foundation under the designed tectonic plate vibration conditions during an earthquake, and make sure the safety factor of the bearing capability under earthquake conditions is $FS_E \geqq 1.2$.

Table 4. Comparison of prevention methods for conventional soil liquefaction and localizations of soil liquefaction.

The prevention methods for conventional soil liquefaction and those for localizations of soil liquefaction are summarized in **Table 4**. It is apparent that the prevention methods provided by the Construction and Planning Agency of the Ministry of the Interior [23] for conventional soil liquefactions are totally different from those for localizations of soil liquefaction. Since the prevention methods for conventional soil liquefaction only take into account the vibration effect, buildings will collapse under the action of shear banding. To diminish the threat of soil liquefaction to buildings, it is necessary to separate shear banding soil liquefaction areas and non-shear banding liquefaction areas, and then provide necessary prevention methods for these two different areas individually.

5. Conclusions

Presently, tectonic earthquakes are known as the most hazardous type of earthquake. The primary effects of tectonic earthquakes are shear bands, followed by seismic vibrations. However, recent earthquake resistance design, verification tests, and liquefaction potential evaluations all focus on seismic vibration. Thus, buildings cannot be completely protected from damage during a tectonic earthquake. Furthermore, the disasters' cause is not appropriately identified. With this in mind, the phenomena occurring during a tectonic earthquake are listed: shear bands, highly concentrated excess pore water pressure, and seismic vibration. Then, the primary role of shear banding in earthquake disasters is discussed. With reference to case studies of earthquake disasters, the author draws the following three conclusions:

1. Collapsed bridges only occur locally in an earthquake and are caused by the dislocations of shear bands induced by localized deformation. When seismic vibration is the only focus of the bridge earthquake-resistance design standard, a rebuilt bridge would still be damaged under the effects of shear band dislocations, even though a dramatic improvement of the seismic vibration resistance has been implemented.
2. If a construction site is located on a leveled shear band slope, when shear band dislocations occur during a tectonic earthquake, buildings may collapse due to the presence of the shear bands. Water pipes beneath the roads could burst due to shear band dislocations, and buildings next to the burst water pipes could also collapse, since the basement walls lose lateral support.
3. Recent soil liquefaction potential diagrams are drawn based on all-around seismic vibrations. For countries on the earthquake band, if areas have a similar alluvial sand soil content, similar groundwater table depths, and similar earthquake magnitudes, those areas will have the same liquefaction potentials. Since soil liquefaction only occurs during tectonic earthquakes, and can be only induced by highly concentrated excess pore water pressures in shear bands, current conventional soil liquefaction potential diagrams do correspond with the localizations of soil liquefaction. Furthermore, soil liquefaction prevention methods based on all-around seismic vibrations can enhance a building's foundation bearing capacity, but cannot eliminate the shear banding effects. In this regard, only by applying prevention methods based on localizations of soil liquefaction can the damage induced by soil liquefaction be effectively alleviated.

Acknowledgements

The previous work of this research is a part of the preliminary studies on the stability of existing earth structures as part of the Repair, Evaluation, Maintenance, and Rehabilitation Research Program (REMR). Financial support provided by the office of Chief of Engineers, U. S. Army, is acknowledged with thanks. Close consultation with Dr. S. K. Saxena and Dr. J. F. Peters was of great benefit in determining the results of the computer analyses. The chance to use the computer facilities in the U. S. Army Engineer, Waterways Experiment Station to finish most of the computer work in this research is highly appreciated.

Author details

Tse-Shan Hsu

Address all correspondence to: tshsu@fcu.edu.tw

Department of Civil Engineering, Feng-Chia University, Taichung, Taiwan

References

[1] China Earthquake Disaster Prevention Center: How do earthquakes happen? Type of earthquakes. China Digital Science and Technology Museum: Earthquake. Available from: http://amuseum.cdstm.cn/AMuseum/earthquak/1/2j-1-2.html

[2] Drucker DC. Some implications of work hardening and ideal plasticity. Quarterly of Applied Mathematics. 1950;**7**(4):411-418. DOI: 10.1090/qam/34210

[3] Hill R. A general theory of uniqueness and stability in elastic-plastic solids. Journal of the Mechanics and Physics of Solids. 1958;**6**:236-249. DOI: 10.1016/0022-5096(58)90029-2

[4] Mandel J. Stability conditions and Drucker's postulate. Translated from "conditions de stabilite et postulat de Drucker". In: Krautchenko J, Sirieys PM, editors. Rheology and Soil Mechanics. Berlin: Springer-Verlag; 1966. DOI: 10.1007/978-3-642-46047-0

[5] Rice JR. The localization of plastic deformation. In: Koiter WT, editor. Proceedings of the 14th International Congress on Theoretical and Applied Mechanics; 1976; Delft, Holland. p. 207-220. ISBN: 0720405491. Available from: http://esag.harvard.edu/rice/062_Rice_LocalPlasDef_IUTAM76.pdf

[6] Rudnicki JW, Rice JR. Conditions for the localization of deformation in pressure-sensitive dilatant materials. Journal of the Mechanics and Physics of Solids. 1975;**23**:371-394. DOI: 10.1016/0022-5096(75)90001-0

[7] Valanis KC. Banding and stability in plastic materials. Acta Mech. 1989;**79**:113-141 Available from: https://link.springer.com/article/10.1007/BF01181483

[8] Hsu TS, Tsao CC, Lin CT. Localizations of soil liquefactions induced by tectonic earthquakes. The International Journal of Organizational Innovation. 2017;**9**(3):110-131 Available from: https://search.proquest.com/docview/1854173598?pq-origsite=gscholar

[9] Lambe TW, Whitman RV. Soil Mechanics. Chichester: John Wylie & Sons; 1972. p. 65

[10] Huang H, Lian Y. The Earth Crack: Taiwan 921 Jiji Earthquake, Bird's Eye View of Cher-Lung-Pu Fault. Sino-Geotechnics Research and Development Foundation. 1999; p. 56 (In Chinese). Available from: http://www.eslite.com/Search_BW.aspx?query=%E5%A4%A7%E5%9C%B0%E8%A3%82%E7%97%95

[11] Google Earth. 2017. Available from: https://www.google.com.tw/intl/zh-TW/earth/download/gep/agree.html

[12] Chen JZ. Open to traffic only two months after reconstruction, pile cap of the Jianmin bridge is exposed. Liberty Times Net. 2012 (In Chinese) Available from: http://news.ltn.com.tw/news/local/paper/606589

[13] Luo P. Aero-snapshot image of the Weiguan building. Liberty Times Net. 2016 (In Chinese) Available from: http://news.ltn.com.tw/news/life/breakingnews/1620861

[14] Liu GY. Seismic damage evaluation and countermeasure study of people's livelihood system (NCREE-07-057). In: Proceedings of Conference on the Chinese Taipei Earthquake Loss Estimation System (TELES). Taipei: National Center for Research on Earthquake Engineering; 2007 (In Chinese)

[15] Hsu TS, Qiu SE, Hong SE, Yen CM. The effect of shear bandings on the burst of trunk pipes. In: Proceedings of the 39th National Conference on Theoretical and Applied Mechanics, CTAM2015-1168. 13 November, 2015; National Taiwan University of Science and Technology (In Chinese)

[16] Apple Daily, Schematic diagram on the deep submersion of block A during the collapse of Weiguan building (In Chinese). 2016. Available from: http://apple.nextmedia.tw/news/local /20160213/3484 6087/privacy

[17] Central Geological Survey, MOEA. Integrated Geological Data Inquiry System. 2017 (In Chinese). Available from: http://www.moeacgs.gov.tw/app/index.jsp

[18] Central Weather Bureau, Ministry of Transportation and Communications. Disastrous earthquakes. 2017 (In Chinese). Available from: http://www.cwb.gov.tw/V7/earthquake/damage_eq.htm

[19] Central Geological Survey, MOEA. Soil Liquefaction Potential System. 2016. Available from: http://www.geologycloud.tw/map/liquefaction/zh-tw

[20] Terzaghi K, Peck RB. Soil Mechanics in Engineering Practice. 2nd ed. Chichester: John Wiley & Sons; 1967. pp. 169-173 ISBN: 9780471086581

[21] Hsu TS, Chiu SE. Piping failure induced by shear bandings: Take the Renyitan reservoir spillway as an example. The International Journal of Organizational Innovation. 2017;**9**(2):239-259 Available from:http://eds.a.ebscohost.com/eds/pdfviewer/pdfviewer?vid=0&sid=8a59d914-6eda-4d84-919a-519090337e01%40sessionmgr4006

[22] Liu J, Lin S. Tough grass, Strong earthquake cannot collapse. China Times, Photography taken by Li T. 2013. Available from: http://www.chinatimes.com/newspapers/20130526000325-260102

[23] Construction and Planning Agency of Ministry of the Interior. Soil liquefaction prevention area. Available from: http://www.cpami.gov.tw/%E6%9C%80%E6%96%B0%E6%B6%88%E6%81%AF/%E6%A5%AD%E5%8B%99%E6%96%B0%E8%A8%8A/19652-%E5%9C%9F%E5%A3%A4%E6%B6%B2%E5%8C%96%E9%98%B2%E6%B2%BB%E5%B0%88%E5%8D%80.html

IntechOpen